Research article

NMR IN BIOMEDICINE

Received: 22 November 2013, Revised: 13 June 2014, Accepted: 10 July 2014, Published online in Wiley Online Library: 14 August 2014

(wileyonlinelibrary.com) DOI: 10.1002/nbm.3177

MRS water resonance frequency in childhood brain tumours: a novel potential biomarker of temperature and tumour environment

Ben Babourina-Brooks[a,b]*, Martin Wilson[a,b], Theodoros N. Arvanitis[b,c], Andrew C. Peet[a,b] and Nigel P. Davies[a,d]

^{1}H MRS thermometry has been investigated for brain trauma and hypothermia monitoring applications but has not been explored in brain tumours. The proton resonance frequency (PRF) of water is dependent on temperature but is also influenced by microenvironment factors, such as fast proton exchange with macromolecules, ionic concentration and magnetic susceptibility. ^{1}H MRS has been utilized for brain tumour diagnostic and prognostic purposes in children; however, the water PRF measure may provide complementary information to further improve characterization. Water PRF values were investigated from a repository of MRS data acquired from childhood brain tumours and children with apparently normal brains. The cohort consisted of histologically proven glioma (22), medulloblastoma (19) and control groups (28, MRS in both the basal ganglia and parietal white matter regions). All data were acquired at 1.5 T using a short T_E (30 ms) single voxel spectroscopy (PRESS) protocol. Water PRF values were calculated using methyl creatine and total choline. Spectral peak amplitude weighted averaging was used to improve the accuracy of the measurements. Mean PRF values were significantly larger for medulloblastoma compared with glioma, with a difference in the means of 0.0147 ppm ($p < 0.05$), while the mean PRF for glioma was significantly lower than for the healthy cohort, with a difference in the means of 0.0061 ppm ($p < 0.05$). This would suggest the apparent temperature of the glioma group was ~1.5 °C higher than the medulloblastomas and ~0.7 °C higher than a healthy brain. However, the PRF shift may not reflect a change in temperature, given that alterations in protein content, microstructure and ionic concentration contribute to PRF shifts. Measurement of these effects could also be used as a supplementary biomarker, and further investigation is required. This study has shown that the water PRF value has the potential to be used for characterizing childhood brain tumours, which has not been reported previously. © 2014 The Authors. *NMR in Biomedicine* published by John Wiley & Sons, Ltd.

Keywords: MRS; thermometry; brain tumours; paediatric; MRI; clinical; brain temperature; proton resonance frequency

INTRODUCTION

Cancer is the most common cause of death in children after infancy, and, whilst significant advances have been made, the rate of improvement in survival is decreasing. Novel techniques are required to continually improve the outcome of cancer patients. One technique is ^{1}H MRS, which is a powerful non-invasive tool for the assessment of childhood brain tumours through MRS pattern classification (1). A complementary analysis technique, which may provide additional information, is ^{1}H MRS thermometry. ^{1}H MRS thermometry is a non-invasive method to measure brain temperature changes and provide information about the tissue microenvironment.

Temperature has been shown to be an important factor in characterizing tumours, with changes in temperature compared with surrounding tissue being observed for different tumour types (2). Infrared thermal imaging has been used as a screening tool for malignant breast tumours (3) and for intra-operatively delineating the margins of brain tumours (2). Temperature rises have been attributed to abnormalities in vasculature leading to hypoxia and abnormal energy metabolism (4,5), whilst decreases may be associated with the presence of necrosis. Hypoxia has been shown to increase treatment resistance in brain tumours, stimulating interest in non-invasive markers of hypoxia to aid prognosis and treatment stratification. The link between hypoxia,

* *Correspondence to: B. Babourina-Brooks, School of Cancer Sciences, University of Birmingham, Birmingham, West Midlands, UK. E-mail: b.brooks@bham.ac.uk*

a *B. Babourina-Brooks, M. Wilson, A. C. Peet, N. P. Davies*
School of Cancer Sciences, University of Birmingham, Birmingham, West Midlands, UK

b *B. Babourina-Brooks, M. Wilson, T. N. Arvanitis, A. C. Peet*
Children's Hospital NHS Foundation Trust, Birmingham, West Midlands, UK

c *T. N. Arvanitis*
Institute of Digital Healthcare, WMG, University of Warwick, Coventry, UK

d *N. P. Davies*
Imaging and Medical Physics, University Hospitals Birmingham NHS Foundation Trust, Birmingham, West Midlands, UK

Abbreviations used: *PRF, proton resonance frequency; NAA, N-acetylaspartate; PRESS, point resolved single voxel spectroscopy; BG, basal ganglia; WM, white matter; A^2_w, spectrum peak amplitude-squared weighting; Cho, total choline; Cr, methyl creatine; $\delta_{W(metabolite)}$, water PRF; $\delta^2_A w$, amplitude-squared weighted water PRF; SD, standard deviation; SNR, signal to noise ratio; PC, phosphocholine; GPC, glycerophosphocholine.*

The copyright line for this article was changed on 29 January 2015 after original online publication.

temperature and metabolism provides an opportunity for non-invasive MR thermometry in combination with MRS to increase the clinical utility of routine MRI scans of childhood cancer at diagnosis and follow-up. Many children with brain tumours do not undergo a biopsy, or have residual masses that need to be monitored, making non-invasive methods for the assessment of the tumour microenvironment particularly attractive.

MRS thermometry, using the water proton resonance frequency (PRF), is calibrated against a temperature independent reference metabolite(s). The water PRF shift is linearly dependent on temperature, between 20 and 50 °C, with a coefficient of ~ -0.01 ppm °C^{-1} (6,7). The water PRF has also been found to be affected by the chemical environment, including ionic concentration, protein concentration (chemical exchange) (8,9) and magnetic susceptibility (10–12). These factors may significantly affect the water PRF, and hence the apparent temperature measure; however, the sensitivity of the PRF to the microenvironment could also be used as a supplementary biomarker. Investigating the microenvironment effect is therefore of interest.

Commonly, N-acetylaspartate (NAA) is used as a metabolite reference due to its high signal in brain tissue; however, NAA signal in brain tumours is significantly reduced and therefore not suitable. Total choline (Cho) and methyl creatine (Cr) are prominent singlet peaks in brain tumours and healthy brain, and therefore more appropriate reference metabolites (12). Cho and Cr have been used individually for brain temperature measures (13–15); however, individual metabolite references can incur error in PRF shift measurement. The error can be random, e.g. low signal to noise ratio (SNR) and finite line-width, and non-random, e.g. overlapping nearby metabolite peaks, which leads to fitting error. Combining multiple metabolite peak references by using an amplitude weighting method significantly reduces the random errors (13).

This technique has been shown to be an effective tool for brain temperature mapping (16–18). The non-invasive measurement of brain temperature is favourable for a number of applications where MRS thermometry could be implemented: brain trauma (19), stroke (20) and hypothermia monitoring (14,21). Both non-invasive temperature and tumour environment measures could aid in tumour diagnosis; however, brain tumour water PRF measures have been relatively unexplored, especially in children. In one study investigating tumour MRS thermometry the authors show significant temperature differences among adult brain tumour types (22).

The aim of this study was to investigate the diagnostic potential of the water PRF shifts of paediatric brain tumours on a clinical 1.5 T scanner. Specifically, two common paediatric tumour types (medulloblastomas and gliomas) and deep grey matter (basal ganglia, BG) and white matter (WM) regions in apparently healthy paediatric brain, were investigated and compared. This was achieved through measuring water PRF differences relative to Cho, Cr and peak amplitude weighting methods.

EXPERIMENT

Patients

Patients under 16 years of age undergoing MRI, prior to diagnosis, for a suspected cerebellar tumour, between 1 September 2006 and 31 July 2011 were eligible for this study. A retrospectively selected patient group of 44 children were studied before treatment, which included major surgical resection with the diagnosis confirmed by histopathology. All patients were chosen based on their visually prominent Cho and Cr reference metabolite peaks. This study's patient cohort, after quality control, consisted of 22 glioma tumours (12 male, 10 female; mean (standard deviation, SD) age 9.1 (4.3) years; 14 grade 1, six grade 2, one grade 3 and one grade 4) and 19 medulloblastomas (13 male, six female; mean (SD) age 6.6 (3.4) years, 19 grade 4). Tumours were graded using the WHO grading system (2007). All medulloblastomas were located in the posterior fossa, and the glioma tumours were mostly in the posterior fossa but five were supratentorial tumours. Tumours were grouped into gliomas and medulloblastomas for comparison purposes.

A control group was selected consisting of 28 children (22 male, six female; mean ± SD age 6.2 ± 4.5 years), who underwent investigations for a suspected metabolic disorder but both MRI and MRS were deemed normal in appearance by an experienced radiologist and none of the cases went on to have a metabolic disorder confirmed. The control group data were acquired in two consistent brain regions containing BG grey matter and parietal WM. Ethics approval for the study was granted by the local research ethics committee, and informed parental consent was also obtained.

Data acquisition

All data were taken from studies using a 1.5 T scanner (Siemens Symphony Magnetom, NUM4). Patients were scanned as part of an MRS multicentre study, unoptimized for MR thermometry. The protocol included T_1- and T_2-weighted images of the brain and MRS and T_1-weighted images of the head and spine after administration of contrast agent. MR spectra were acquired using a water suppressed chemical-shift-selective point resolved single voxel spectroscopy (PRESS) sequence ($T_E = 30$ ms, $T_R = 1500$ ms) with an acquisition bandwidth per point of 1.024 Hz. Cubic voxels with 2 cm or 1.5 cm length were used and 128 or 256 repetitions were acquired, respectively. Water reference spectra with eight repetitions were acquired for eddy current correction and as an internal reference for quantifying metabolite concentrations. The conventional images were used to delineate the margins of the primary tumour and enable the placement of the MRS voxel within the solid-appearing component of the tumour (Fig. 1). The risk of lipid contamination of the MRS signal from scalp or other fatty tissue was minimized by avoiding close proximity to these areas during positioning of the voxel.

MRS processing

Spectra were analysed in the jMRUI (jMRUI, Java Magnetic Resonance User Interface) software package using the AMARES tool (23). The Cr and the Cho peak were chosen as references since they were prominent in all tumour and healthy spectra. Mean spectra of the groups, with SD, were generated using MATLAB and normalized by the sum of the absolute real values in the frequency domain (0.5–4 ppm range) (see Figure 3 later).

The PRF of water (δ_{H2O}), choline (δ_{Cho}) and creatine (δ_{Cr}) were determined in the frequency domain by correcting the zero order phase manually and fitting individual peaks with a Lorentzian profile. Chemical shifts of 4.68 ppm, 3.03 ppm and 3.22 ppm were used as initial estimates for fitting the H_2O, Cr and Cho peaks respectively. Since NAA was not often readily detected in all tumour spectra, only water PRF shifts relative to Cr, $\delta_{(H2O\ -\ Cr)}$, and Cho, $\delta_{(H20\ -\ Cho)}$, were determined for each spectrum (Fig. 2).

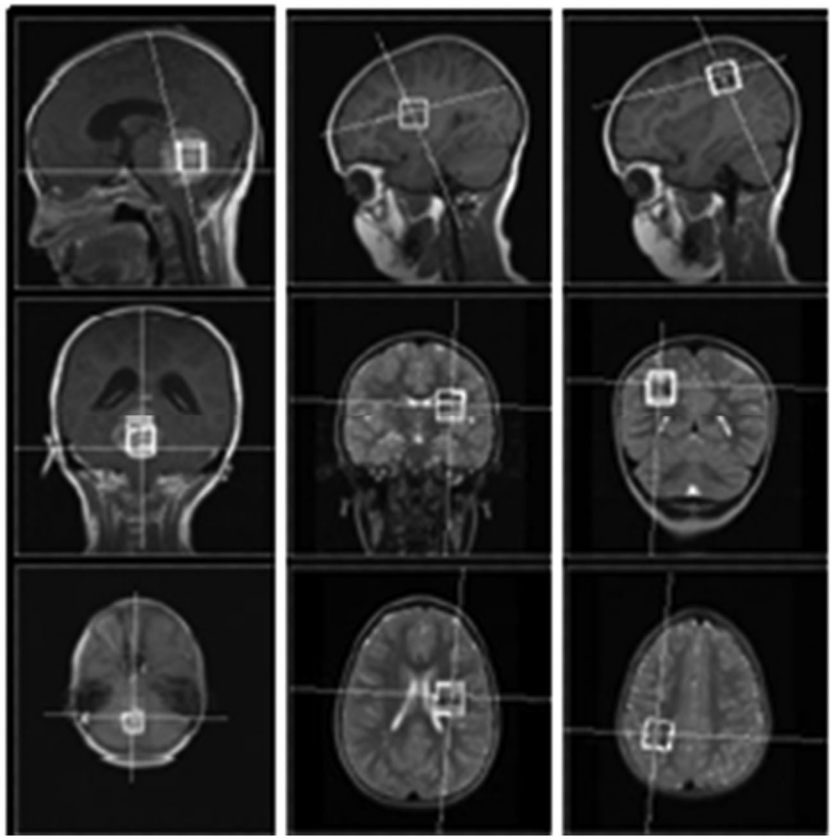

Figure 1. Voxel placements of a grade 1 glioma (left), BG (centre) and WM (right) regions in a patient and two different controls, respectively.

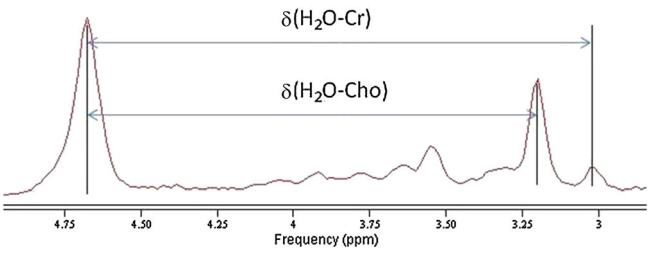

Figure 2. A low grade glioma tumour spectrum depicting the water peak to reference metabolite chemical shift measure.

To standardize the inherently different metabolite shifts, $\delta_{(H2O\ -\ Cho)} \approx 1.46$ ppm and $\delta_{(H2O\ -\ Cr)} \approx 1.65$ ppm, standardized water PRF values were calculated using Equation [1]. Converting the PRF shift to temperature may also provide a standardized value; however, an absolute temperature value requires calibration for each tissue structure based on other factors affecting the PRF (9), e.g. fast proton exchange. Therefore, the calculated water PRF value was deemed more appropriate as the quantity to report in this study.

The water PRF ($\delta_{W(metabolite)}$) was calculated by summing the measured $\delta_{(H2O\ -\ metabolite)}$ and a set constant PRF value for the reference metabolites, Cho = 3.22 ppm, Cr = 3.03 ppm, labelled $\delta_{set\ metabolite}$ in Equation [1]. This value relates to the water chemical shift, allows comparison between metabolite references and reduces bias arising from the shift difference when calculating amplitude weighted PRF shifts.

$$\delta_{w(metabolite)} = \delta_{(H2O-metabolite)} + \delta_{set\ metabolite} \quad [1]$$

The error in $\delta_{W(metabolite)}$ is inversely proportional to the reference peak amplitude; therefore, an average value for multiple reference metabolites weighted by the square of the reference peak amplitude provides a more precise PRF measure (13,24). Therefore, reference peak amplitude-squared weighting (A_w^2) was used (12). The A_w^2 equation is

$$\delta_{AW}^2 = \frac{\left(\delta_{W(Cho)}A_{Cho}^2 + \delta_{W(Cr)}A_{Cr}^2\right)}{A_{Cho}^2 + A_{Cr}^2} \quad [2]$$

The mean (SD) of the water PRF ($\delta_{W(metabolite)}$) and $A^2{}_w$ water PRF (δ_{AW}^2) were calculated for each spectrum.

SNR was defined as the reference metabolite signal amplitude divided by the SD of the noise. Individual peak, Cho and Cr, SNRs were calculated and compared for all groups (see Table 1 later).

Quality control

Two quality control criteria were applied to the spectra: (1) FWHM of the water reference peak less than 10 Hz and (2) SNR

Table 1. Individual reference peak, Cho and Cr, SNR values and SDs for the studied patient groups

Patient group	Cho mean SNR (SD)	Cr mean SNR (SD)
Medulloblastoma	9.1 (4.4)	3.4 (1.4)
Glioma	6.5 (2.9)	3.6 (1.7)
BG	3.6 (0.9),	4.8 (0.9)
WM	3.9 (1.2)	3.3 (0.8)

of the metabolite spectra greater than four. Spectrum fits were individually screened for artefacts and baseline anomalies. Individual metabolite fits produced by AMARES were also inspected to confirm that they corresponded to the features seen in the tumour spectra. In particular the Cho and Cr, at PRFs of 3.22 ppm and 3.03 ppm respectively, were assessed. Based on the selection criteria only three of the selected spectra were rejected.

Statistical analysis

Comparisons of the mean PRF between the four groups, medulloblastomas, gliomas, control BG and WM, were made using pairwise two-tailed Student *t*-tests. The threshold for significance was taken as $p < 0.05$. A power analysis calculation showed that the 19 samples would detect a large effect size (Cohen $d = 0.68$) for a two-tailed, paired *t*-test at a significance level of 0.05 with a power of 0.80.

RESULTS

The mean (SD) water line-width and metabolite SNR across the accepted tumour cases were 5.1 (1.6) Hz and 8.0 (4.5), respectively.

The mean spectra had distinct Cho and Cr peaks in both healthy and tumour cases (Fig. 3). The NAA peak was poorly defined in tumour spectra due to its low signal intensity and overlap with signals from glutamate, glutamine and macromolecules increases fitting error. Cho and Cr were used as metabolite references to give the most accurate PRF shift for groups chosen. The individual peak SNR values (SD) are shown in Table 1.

The average Cho/Cr ratio was 1.54 (2.35), 2.52 (2.64), 1.32 (0.23) and 0.85 (0.21) for the medulloblastoma, glioma, BG and WM, respectively. Therefore, the spectral peak amplitude-squared weighting of the water PRF was substantially weighted towards the Cho peak value, except in the WM group.

Spectral peak amplitude-squared weighted water PRF shift

The δ_{A^2W} mean (SD) values for the medulloblastoma, glioma, BG and WM groups were 4.689 ppm (0.011 ppm), 4.674 ppm (0.014 ppm), 4.684 ppm (0.0083 ppm) and 4.683 ppm (0.013 ppm), respectively (Fig. 4). The medulloblastoma δ_{A^2W} was significantly higher than the δ_{A^2W} of the glioma group, with a difference of 0.0147 ppm, $p < 0.01$. However, it was similar to that in the BG or WM group, $p \sim 0.09$, with differences of 0.0053 ppm and 0.0061 ppm, respectively. The glioma group δ_{A^2W} was 0.0094 ppm lower than for the BG, $p < 0.01$, and 0.0086 ppm lower than the WM group value, $p < 0.05$.

Individual metabolite based water PRF

Comparison of the individual water PRF shifts, $\delta_{W(Cho)}$ and $\delta_{W(Cr)}$ (Fig. 5) shows a similar trend, across the groups, to the amplitude-squared weighted results (Fig. 4). However, the SD was generally larger for the water PRF shifts calculated using individual metabolite references. Comparing the two individual

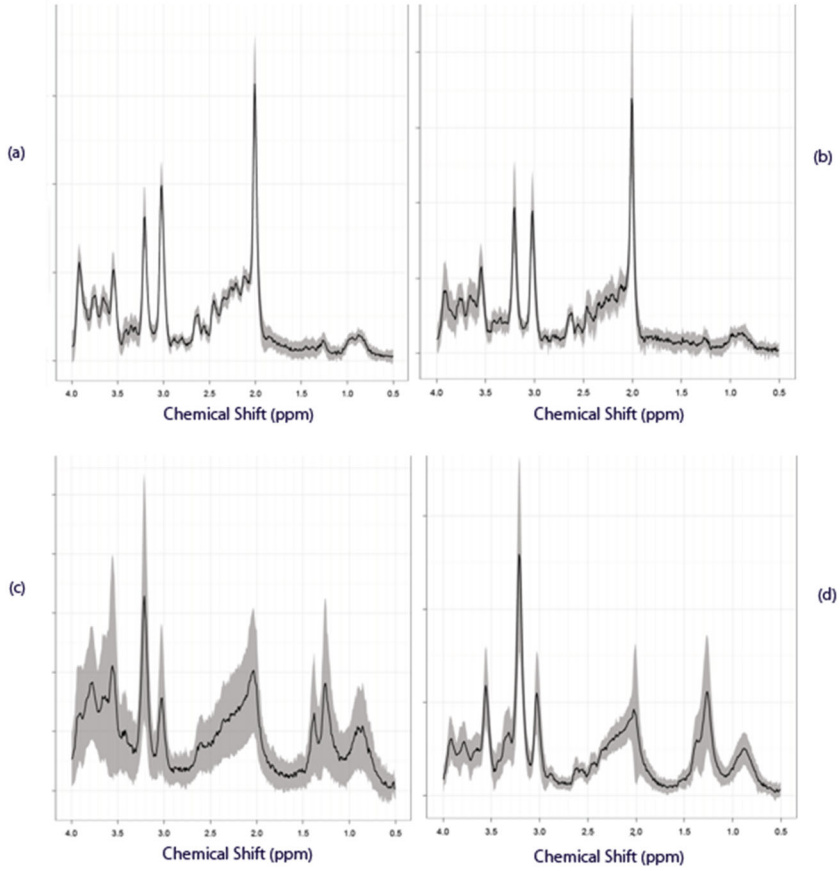

Figure 3. Mean metabolite spectra of tumour and control brain cohorts: (a) control BG, (b) control WM, (c) glioma and d) medulloblastoma regions. Standard deviations are shown via grey bands.

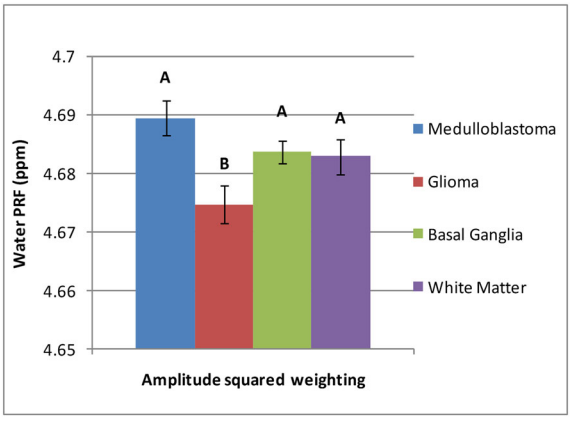

Figure 4. Mean (standard error) amplitude-squared weighted water PRF values for the patient cohorts. Means with different letters are significantly different ($p < 0.05$, A–B $p < 0.01$).

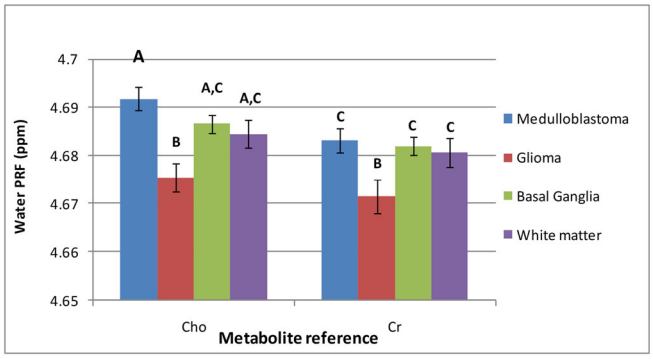

Figure 5. Mean (standard error) choline and creatine based water PRF values for the patient cohorts. Means with different letters are significantly different ($p < 0.05$, A–B $p < 0.01$); A,C was not significantly different from A or C.

metabolite reference plots, the Cr plot had consistently reduced mean PRF values across groups; however, only the medulloblastoma group PRF difference was significant, $p < 0.05$. The group SDs were similar for each individual metabolite reference, except for the glioma group, in which the SD for $\delta_{W(Cr)}$ was significantly larger, $p < 0.05$.

Apparent temperature

Apparent temperature conversions were based on healthy piglet brain temperature calibrations, which were reported to represent central brain temperature in humans well, for Cho and Cr individually (8). The mean apparent temperatures were 35.8 °C, 37.2 °C, 36.3 °C and 36.5 °C for the medulloblastoma, glioma, BG and WM groups, respectively, using the Cho metabolite reference. When Cr was used as the reference the results were 35.7 °C, 36.4 °C, 35.5 °C and 35.6 °C for the medulloblastoma, glioma, BG and WM groups, respectively.

The apparent temperature mean values were different between the tumour groups and in gliomas compared with grey and white matter in the control group, $p < 0.05$. The mean apparent temperature was significantly lower in the medulloblastoma group compared with the control group, but only when using Cho as the reference metabolite, $p < 0.05$. The apparent temperature using Cho as the reference metabolite was always higher than that calculated using Cr as the reference, although for the medulloblastoma group the values were comparable.

DISCUSSION

In this study, the PRF of water was investigated based on two reference metabolites, Cho and Cr. The δ_{A^2W} shifts were observed for different cohorts consisting of two childhood brain tumour types and two brain regions in a group of children with apparently normal brain spectra as control groups. Significant differences were observed between the tumour groups and between the tumour and control groups. The δ_{A^2W} was significantly different for the medulloblastoma and glioma tumour types in this study; however, elucidating the mechanisms underlying the shift difference will be essential to unlocking the technique's potential.

The results of this study are based on clinical data taken from routine MRS scans. The measure of the water PRF shift is therefore a free measure complementary to MRS metabolite concentrations and profiling.

Spectrum-peak amplitude-squared weighted water PRF shift

The control cohort δ_{A^2W} was not significantly different from the initial estimate of 4.68 ppm. However, the PRF shift of the tumour groups compared with the control cohort was higher for the medulloblastoma group and lower for the glioma group. Assuming that a major contribution to the PRF change is temperature, the water PRF shift of the medulloblastoma group would imply a lower mean temperature than for the glioma group.

Models of temperature change due to metabolic activity and blood flow have been investigated in healthy brain (24). Mean temperature differences of ~0.3 °C were calculated between tissue and blood temperature in resting state healthy brain. However, tumour vasculature and metabolic rates are different, hence a larger temperature difference may be seen depending on the tumour physiology and metabolism. Metabolic rate and blood flow may therefore be a major cause for temperature differences between tumour types. A difference in mean temperature may arise from differences in cellularity, necrosis, hypoxia and vasculature between the two tumour groups. High cellularity with increased metabolic rate and hypoxic regions (high metabolism and low blood flow) may be expected to lead to higher average temperature, while necrotic regions and increased vascularity may be expected to lead to lower average temperature due to reduced metabolism and increased thermal transportation from the tumour respectively. Medulloblastomas are highly cellular compared with low grade gliomas, and they have relatively small amounts of necrosis and hypoxia compared with high grade gliomas (26). Necrotic regions were also avoided as much as possible in the placement of the spectroscopy regions of interest. Therefore, active cell density and vascularity are expected to be the main drivers for the possible temperature differences seen in this study. A lower temperature in medulloblastomas could be explained by increased thermal transport effects outweighing any increased metabolic activity (26,27). Indeed, in comparison with the glioma group, consisting of mainly low grade tumours, the medulloblastomas are known to have increased vasculature that could provide a cooling effect (28). However, due to competing drivers for temperature change

NMR IN BIOMEDICINE

in the tumour groups and the sensitivity of the water PRF to other factors, it is unlikely that all of the difference in water PRF observed can be explained by temperature effects.

An increase in temperature lengthens the hydrogen bonding between molecules, which increases the electron shielding, thereby decreasing the water PRF (29,30). The temperature measure in tumours may be of importance, particularly if a link with hypoxia can be verified. Hypoxic tumours resist radiotherapy treatment, and non-invasive measures of hypoxia would be advantageous for treatment stratification. However, changes in the water PRF may also relate to tissue environment differences. The difference in the water PRF shift observed could have significant contributions from chemical environmental effects such as protein and ionic concentration, cellular structure, tissue water content, pH (7,9,17) and magnetic susceptibility effects (11). Such environmental factors can be quite different between tumour types, hence associated water PRF changes could provide a unique measure to aid characterization. However, elucidating the individual contributions of temperature and tissue environmental factors to the water PRF shift requires further investigation.

The water PRF shift has been shown to be directly proportional to protein concentration *in vitro* (8,9). This is due to fast chemical exchange between free water and bound macromolecular protons. The magnitude of this effect on water PRF *in vivo* will depend on water content, macromolecular concentration and microstructure. An increase in the fast chemical exchange effect would result in an increased water PRF and a decreased apparent temperature. In medulloblastomas, necrosis is relatively low and cellularity is high compared with the mainly low grade gliomas. This is likely to mean increased fast chemical exchange effects in the medullobastomas and consequently an increased water PRF, which could explain the results of this study. The BG and WM have similar PRF values, as expected due to good thermoregulation in the brain (25,31) and similar protein concentrations and water contents (32,33).

Ionic concentration has been shown to decrease the water PRF shift (9), which mimics an increased temperature and opposes the fast chemical exchange effect. Ionic concentrations in tumour and healthy tissue have been measured using ^{23}Na spectroscopy (34). The results are a measure of the combined extracellular and intracellular ionic concentrations, which is relevant to ^{1}H MRS as it also measures the average of both compartments. Adult malignant glioma tumour tissue was found to have a sodium concentration of 103 (36) mM/kg, compared with healthy tissue, which had approximately 65 (9) mM/kg. Therefore, this increased ionic concentration would result in an increased apparent temperature. In this study, a reduced PRF shift was seen for the gliomas compared with healthy tissue, which may have substantial contributions from increased temperature and ionic concentration. In adult healthy brain, GM and WM groups, the ionic concentrations have been shown to be similar (34). Childhood tumour types may have significantly different ionic concentrations but the authors are unaware of any studies that have investigated this.

Other potential explanations for the difference in water PRF seen between the tumour groups include magnetic susceptibility effects due to tissue heterogeneity on both macroscopic and cellular scales. Where the water and metabolite compartments are not perfectly co-located, it is possible that such effects may not be adequately accounted for simply by referencing to temperature insensitive metabolite peaks. On a macroscopic level this may be caused by chemical shift displacement or by significant amounts of cystic or necrotic material within the voxel. Microscopic susceptibility effects on the water PRF may result from a combination of anisotropic tissue microstructure and differences in the cellular distribution of the Cho and Cr metabolites and the water (10). However, this study was undertaken at a field strength of 1.5 T and care was taken to avoid cystic or necrotic areas within the voxels, hence both the macroscopic and microscopic magnetic susceptibility effects are thought to have had a small or negligible impact in this study. However, such effects may be more significant at higher field strengths and should be considered in future studies.

pH may also be of importance for water PRF measures *in vivo*, as tumour extracellular space is more acidic compared with healthy tissue (35); however, several *in vitro* studies have shown no significant effect of pH on water PRF (7,17,36,37).

Individual reference metabolite based water PRF

While spectrum peak amplitude-squared weighting of multiple reference metabolites provides improved accuracy and precision of the water PRF value, the measurements based on each individual reference metabolite may contain interesting information and reveal subtle differences between the groups. $\delta_{W(Cr)}$ values were generally lower than $\delta_{W(Cho)}$ for all groups (Fig. 5). Both reference peaks have contributions from more than one metabolite; however, at 1.5 T they are unresolved and form a single peak. Each contributing metabolite has a slightly different PRF and therefore may affect the average PRF of the reference metabolite. Davies *et al.* used high resolution magic angle spinning spectroscopy to investigate the free choline ($\delta \sim 3.205$ ppm), phosphocholine (PC, $\delta \sim 3.225$ ppm) and glycerophosphocholine (GPC, $\delta \sim 3.233$ ppm) contributions to Cho in childhood tumour tissue (1). The contribution to the Cho PRF from PC is large in medulloblastomas and significantly less in gliomas. The GPC contribution is small in medulloblastomas but large in gliomas. The free choline contribution appears to be small for both tumour groups. Since we used a fixed reference value of 3.22 ppm for Cho, this would result in an apparent water PRF difference between medulloblastomas and gliomas, which is estimated to be ~0.0035 ppm. This could explain approximately 20% of the difference in water PRF between the tumour groups in this study.

Total creatine (Cr) comprises creatine and phosphocreatine; however, the signals are only 0.002 ppm apart and their concentration across cohort groups is similar (1); therefore, this would not significantly affect the water PRF measurement. Cr would seem to be a more consistent reference metabolite; however, compared with Cho the concentration in tumours is lower and the variation in concentration is larger, even within the same tumour group. This promotes larger relative contributions from nearby metabolites and noise, increasing measurement error. This was reflected in the larger SDs observed for the Cr referenced water PRFs than for Cho referenced water PRFs in this study. Individual reference metabolite chemical shift differences were also seen in healthy piglet brain by Cady *et al.* (13). Their results were consistent with a lower PRF shift for Cr metabolite reference measures. This was attributed to the presence of multiple metabolites in the Cho peak; however, this does not explain all the differences in this work. Further work is required to understand the difference observed in water PRF when using the two individual reference metabolites.

Apparent temperature

The authors are not aware of any studies reporting brain tumour temperature differences in children in the literature; however, one study investigated this in adults. Their study found a significant difference between two adult brain tumour groups, glioma and meningioma (22). The mean low grade glioma apparent temperature (37.0 °C) found in this study was different from their result, 36.0 °C. This can be explained by their use of a different single reference metabolite, NAA, a different calibration equation (7) and biological differences in the tumour types in adults compared with children. NAA concentration is relatively small in a range of tumour types, which may introduce errors in peak fitting and therefore PRF shift. By using two metabolites and averaging the shifts, the PRF error due to small metabolite concentration may be reduced (13).

Overall, the apparent temperature is a combination of actual temperature and micro-environmental effects as previously described. The influence of the micro-environmental effects on the water PRF measure is of great interest due to the importance of the tumour micro-environment for characterizing tumour types and predicting response to treatment.

Limitations

The selection criteria were based on prominent Cho and Cr peaks, which created a selection bias towards higher SNR spectra. A prospective study including consecutive brain tumour patients to evaluate the effect of varying spectral quality would be of interest. The control group had apparently normal spectra, but there may be subtle differences between our control group and healthy volunteers; however, the chance of this significantly affecting the results presented here is low.

The power analysis showed the number of patients included was sufficient to detect significant differences between tumour groups. The SDs, which reflect both the measurement uncertainty and the between-subject variability for each group, were small enough to observe differences between most groups, although the medulloblastoma group was not significantly different from the healthy groups. This difference may become significant with higher spectral resolution and/or SNR to reduce measurement uncertainty, particularly for the lower amplitude Cr reference. Such improvements in metabolite-referenced water PRF measurements could be achieved by performing studies at higher field strength, without a necessary increase in acquisition time. Future studies should take advantage of the increasing use of 3 T scanners for childhood brain tumour imaging to exploit this expected increase in precision, while accounting for the associated increase in magnetic susceptibility and chemical shift displacement effects.

CONCLUSION

The water PRF shift was shown to differ between two major paediatric tumour types, gliomas and medulloblastomas, based on mean cohort values. This suggests that the water PRF has the potential to characterize tumours. Further work may identify the separate contributions from temperature and micro-environmental effects on the water PRF measure, which could provide further aid in diagnosis and prognosis for childhood brain tumours.

Acknowledgements

We would like to thank the staff of the Radiology Department at Birmingham Children's hospital for their help in collecting the MRS data. We would also like to thank Jane Crouch for co-ordinating the study, Rachel Grazier for data management and Cay Shakespeare for patient and parent liaison.

Sponsors: Birmingham Hospital Charities, grant number DJAA RCPF15785. CR UK and EPSRC Cancer Imaging Programme at the Children's Cancer and Leukaemia Group (CCLG) in association with the MRC and Department of Health (England) (C7809/A10342). NIHR Research Professorship (AP, MW), NIHR/CSO Healthcare Scientists Research Fellowship (ND) and EU Marie Curie: International Incoming Fellowship (BB).

REFERENCES

1. Davies NP, Wilson M, Harris LM, Natarajan K, Lateef S, Macpherson L, Sgouros S, Grundy RG, Arvantis TN, Peet AC. Identification and characterisation of childhood cerebellar tumours by *in vivo* proton MRS. NMR Biomed. 2008; 21: 908–918.
2. Kateb B, Yamamoto V, Yu C, Grundfest W, Gruen JP. Infrared thermal imaging: a review of the literature and case report. Neuroimage 2009; 47(S2): 154–162.
3. Head JF, Wang F, Lipari CA, Elliot RL. The important role of infrared imaging in breast cancer. IEEE Eng. Med. Biol. Mag. 2000; 19(2): 52–57.
4. Karaszewski B, Wardlaw JM, Marshall I, Cvoro V, Wartolowska K, Haga K, Armitage PA, Bastin ME, Dennis MS. Early brain temperature elevation and anaerobic metabolism in human acute ischemic stroke. Brain 2009; 12(4): 1093–1102.
5. Yetkin FZ, Mendelsohn D. Hypoxia imaging in brain tumours. Neuroimaging Clin. N. Am. 2002; 12(4): 537–552.
6. Hindman JC. Proton resonance shift of water in the gas and liquid states. J. Chem. Phys. 1966; 44: 4582–4592.
7. Cady EB, D'Souza PC, Penrice J, Lorek A. The estimation of local brain temperature by in vivo 1H magnetic resonance spectroscopy. Magn. Reson. Med. 1995; 33: 862–867.
8. Babourina-Brooks B, Simpson R, Arvanitis TN, Peet AC, Davies NP. An accurate calibration of MRS thermometry at 3T. In: *Proceedings of the 21st Annual Meeting ISMRM, Salt Lake City, USA*. ISMRM, Berkley, USA. 2013; 533.
9. Vescovo E, Levick A, Childs C, Machin G, Zhao S, Williams SR. High-precision calibration of MRS thermometry using validated temperature standards: effects of ionic strength and protein content on the calibration. NMR Biomed. 2013; 26(2): 213–223.
10. Chadzynski GL, Bender B, Groeger A, Erb M, Klose U. Tissue specific resonance frequencies of water and metabolites within the human brain. J. Magn. Reson. 2011; 212(1): 55–63.
11. He X, Yablonskiy DA. Biophysical mechanisms of phase contrast in gradient echo MRI. Proc. Natl. Acad. Sci. U. S. A. 2009; 106(32): 13558–13563.
12. Luo J, He X, d'Avignon A, Ackerman JJ, Yablonskiy DA. Protein-induced water ^{1}H MR frequency shifts: contributions from magnetic susceptibility and exchange effects. J. Magn. Reson. 2010; 202: 102–108.
13. Cady EB, Penrice J, Robertson NJ. Improved reproducibility of MRS regional brain thermometry by 'amplitude-weighted combination'. NMR Biomed. 2010; 24: 865–872.
14. Corbett R, Laptook A, Weatherall P. Non-invasive measurements of human brain temperature using volume-localised proton magnetic resonance spectroscopy. J. Cereb. Blood Flow Metab. 1997; 17: 363–369.
15. Zhu M, Bashir A, Ackerman J, Yablonskiy DA. Improved calibration technique for in vivo proton MRS thermometry for brain temperature measurement. Magn. Reson. Med. 2008; 60: 536–541.
16. Karaszewski B, Wardlaw JM, Marshall I, Cvoro V, Wartolowska K, Armitage PA, Carpenter T, Bastin ME, Farrall A, Haga K. Measurement of regional brain temperature using proton magnetic resonance spectroscopic imaging: validation and application to acute ischemic stroke. Magn. Reson. Imaging 2006; 24: 699–706.

17. Corbett RJT, Laptook AR, Tollefsbol G, Kim B. Validation of a noninvasive method to measure brain temperature in vivo using 1H NMR spectroscopy. J. Neurochem. 1995; 64: 1224–1230.
18. Childs C, Hiltunnen Y, Vidyasagar R, Kaupinnen R. Determination of regional brain temperature using proton magnetic resonance spectroscopy to assess brain–body temperature differences in healthy human subjects. Magn. Reson. Med. 2007; 57: 59–66.
19. Soukup J, Zauner A, Doppenberg EM, Menzel M, Gilman C, Young HF, Bullock R. The importance of brain temperature in patients after severe head injury: relationship to intracranial pressure, cerebral perfusion pressue, cerebral blood flow, and outcome. Neurotrauma 2002; 19: 559–571.
20. Corbett RJT, Purdy PD, Laptook AR, Chaney C, Garcia D. Non-invasive measurement of brain temperature after stroke. Am. J. Neuroradiol. 1999; 20: 1851–1857.
21. Weis J, Covaciu L, Rubertsson S, Allers M, Lunderquist A, Ahlstrom H. Non-invasive monitoring of brain temperature during mild hypothermia. Magn. Reson. Imaging 2009; 27: 923–932.
22. Jayasundar R, Singh VP. In vivo temperature measurements in brain tumours using proton MR spectroscopy. Neurol. India 2002; 50: 436–439.
23. Vanhamme L. Improved method for accurate and efficient quantification of MRS data with use of prior knowledge. J. Magn. Reson. 1997; 129: 35–43.
24. Cavassila S, Deval S, Huegen C, van Ormondt D, Graveron-Demilly D. Cramer–Rao bound expressions for parametric estimation of overlapping peaks: influence of prior knowledge. J. Magn. Reson. 2000; 143: 311–320.
25. Yablonskiy DA, Ackerman JJ, Raichle ME. Coupling between changes in human brain temperature and oxidative metabolism during prolonged visual stimulation. Proc. Natl. Acad. Sci. U. S. A. 2000; 97(13): 7603–7608.
26. Louis DN, Ohgaki H, Wiestler OD, Cavenee WK, Burger PC. The 2007 WHO classification of tumours of the central nervous system. Acta Neuropathol. 2007; 114: 97–109.
27. Holthoff VA, Herholz K, Berthold F, Widemann B, Schroder R, Neubauer I, Heiss WD. In vivo metabolism of childhoof posterior fossa tumors and primitive neuroectodermal tumors before and after treatment. Cancer 1993; 72(4): 1394–1403.
28. Yeom KW, Mitchell LA, Lober RM, Barnes PD, Vogel H, Fisher PG, Edwards MS. Arterial spin-labeled perfusion of pediatric brain tumours. Am. J. Neuroradiol. 2014; 35(2): 395–401.
29. Muller N, Reiter RC. Temperature dependence of chemical shifts of protons in hydrogen bonds. J. Chem. Phys. 1965; 42: 3265–3269.
30. Sare EJ, Moynihan CT, Angell CA. Proton magnetic resonance chemical shifts and the hydrogen bond in concentrated aqueous electrolyte solutions. J. Chem. Phys. 1973; 77: 1869–1876.
31. Banay-Schwartz M, Kenessey A, DeGuzman T, Lajtha A, Palkovits M. Protein-content of various regions of rat-brain and adult and aging human brain. Age 1992; 15: 51–54.
32. Tofts P. *Quantitative MRI of the Brain: Measuring Changes Caused by Disease*. Wiley: Chicester, 2003, pp. 93–97.
33. Paus T, Collins DL, Evans AC, Leonard G, Pike B, Zijdenbos A. Maturation of white matter in the human brain: a review of magnetic resonance studies. Brain Res. Bull. 2001; 54: 255–266.
34. Ouwerkerk R, Jacobs MA, Macura KJ, Wolff AC, Stearns V, Mezban SD, Khouri NF, Bluemke DA, Bottomley PA. Tissue sodium concentration in human brain tumors as measured with ^{23}Na MR imaging. Radiology 2003; 12(2): 529–537.
35. Tannock IF, Rotin D. Acid pH in tumours and its potential for therapeutic exploitation. Cancer Res. 1989; 49: 4373–4384.
36. Peters RD, Hinks RS, Henkelman RM. *Ex vivo* tissue-type independence in proton-resonance frequency shift MR thermometry. Magn. Reson. Med. 1998; 40(3): 454–459.
37. Kanai Y, Nakamura M, Kikuma N, Yasui G, Takada K. Effects of temperature and pH on the chemical shift of metabolites in proton-MRS. Jpn. J. Radiol. Technol. 2001; 57: 651–656.

